

Identifying regions of high drought mortality risk for tree species in NSW

**Final report to New South Wales, Office of
Environment and Heritage,
May 2019**

Project Leads: Belinda Medlyn, Linda Beaumont

**Chief Investigators: David Tissue, Mark Tjoelker, Paul Rymer, Remko Duursma,
Brendan Choat, Tony Auld**

**Contributors: Martin De Kauwe, Chris Blackman, Ximeng Li, John Baumgartner,
Sikdar Rasel**



WESTERN SYDNEY
UNIVERSITY



Hawkesbury Institute
for the Environment

Contents

Executive Summary.....	3
1. Introduction.....	4
2. Species Distribution Models	5
Introduction	5
Method.....	6
Results.....	8
Discussion	10
3. Ecophysiological Experiments	11
Introduction	11
Experiment 1: Stomatal and hydraulic traits	13
Experiment 2: Desiccation time.....	19
Additional experiments.....	21
Development of process-based model.....	22
4. Remote Sensing / Monitoring.....	24
5. General Discussion	24
References.....	25
Appendix 1. Scientific Publications to Date.....	28
Appendix 2. Hydric envelope for 47 tree species	30
Appendix 3. Dry stress for NSW/ACT stands of 47 tree species.....	31
Appendix 4. Maps of dry stress for 47 tree species.....	32

Executive Summary

Drought is well recognised as a major threat to tree survival across Australia. Given the importance of tree species for ecosystem services, and the exposure of the Australian landscape to drought, understanding the risk of drought mortality for key tree species across NSW in current and future climates is vital. We aimed to assess drought mortality risk for a number of tree species common to New South Wales (NSW) forests through three complementary research streams.

Stream one utilised simple species distribution models, termed “hydric envelopes”, and calculated moisture requirements for 47 tree species. This allowed us to identify regions where the 47 species were likely to have been exposed to dry stress during the Millennium Drought (MD, 2000-2009), and under scenarios for the near (2030) and far (2070) future obtained from the NSW and ACT Regional Climate Modelling Program (NARClIM). Findings indicate that populations along species’ western range margins were likely to be under dry stress during the MD, and that future mortality risk may be highest in the central parts of the Great Dividing Range.

Stream two conducted a series of ecophysiological experiments across 12 species, to identify thresholds that lead to hydraulic failure. A key result was that mean annual precipitation across a species’ climate of origin can be used to predict major physiological thresholds, including stomatal closure and the onset of hydraulic failure. In addition, our experiments demonstrate that the desiccation time, an indication of the physiological progression of drought, can be predicted from species traits. Our findings help to identify how these thresholds during drought vary across the landscape, and form a basis for predictions of future mortality risk.

Stream three was tasked with utilising remote sensing to identify mortality events. Ultimately, however, this approach was unsuccessful: current remote sensing capacity is better suited to mapping mortality events that are already known, than identifying new events. Therefore, we determined the need for recording and compiling on-the-ground observations of tree mortality where it occurs. We developed a citizen science website to record tree deaths. Information gathered by this site to date shows that the current drought in SE Australia is causing significant tree death from the Queensland-NSW border down to Tasmania, emphasising the need to continue research into the thresholds for native tree mortality.

1. Introduction

Trees define our landscapes and are crucial for ecosystem services including biodiversity, carbon sequestration and prevention of soil erosion. Drought is a major threat to tree survival across Australia (Mitchell et al. 2014) and is being exacerbated by rising temperatures and changing rainfall patterns due to climate change (CSIRO and BoM, 2018). The goal of this project was to calculate the risk of drought mortality for key tree species across NSW in current and future climates. We aimed to use several complementary research streams to develop risk profiles that account for variation in drought intensity and species resilience over landscapes.

New South Wales forms a scientifically interesting case study for predicting drought mortality risk owing to its east-to-west rainfall gradient. Tree species show strong adaptation to the rainfall environment across this gradient. We chose to study a suite of relatively widespread tree species found in forests and woodlands across this gradient, namely rainforest, wet sclerophyll forest, dry sclerophyll forest, grassy woodlands and semi-arid woodlands.

Most NSW tree species are relatively well-adapted to drought because of the high interannual variability in rainfall (Nicholls et al. 1997). Nonetheless, all are at risk of drought mortality, because previous studies have shown that most species have a small safety margin during drought (Choat et al. 2012). A number of drought mortality events have occurred in NSW in the past (Mitchell et al. 2014), and the drought mortality risk is likely to increase in future as the climate warms. Warmer temperatures tend to increase evaporation rates, increasing the incidence of drought even if rainfall remains unchanged. We used climate projections from the NSW and ACT Regional Climate Modelling project (NARClIM) (Evans et al. 2014; OEH 2014) to determine future drought mortality risk. These projections include four alternative scenarios generated by different climate models (resulting in 12 projections per time period). All scenarios project an increase in temperature in future, but they differ in rainfall projections.

We aimed to assess drought mortality risk for our representative tree species within three complementary research streams. Stream one used simple species distribution models, which assess the relationship between where a species is known to occur and the environmental characteristics (in this case, moisture availability) of those regions. SDM assumes that the environmental tolerances and preferences of a species can be described by the location of its current populations (Franklin 2010; Elith & Leathwick 2009). SDMs can then be used to map the distribution of suitable/unsuitable habitat for the target species and to assess how the suitability of a region can vary over different time periods. In this stream (Section 2), we specifically quantified the breadth of water availability conditions across the set of occurrence records collated for each species, hence assuming that drought mortality risk increases where mean water availability conditions fall below the suitability threshold (Aubin et al. 2018). This approach enabled us to identify regions at increased risk of drought mortality in the alternative future climate scenarios.

The second stream is a process-based ecophysiological approach (Section 3). In this stream, we identified the main underlying mechanisms leading to tree mortality and experimentally quantified thresholds for

these mechanisms for our target species. We have focused on processes leading to hydraulic failure – the collapse of the “plumbing” that transports water from the roots to the leaves. Hydraulic failure has been identified as the most likely mechanism to cause drought mortality in Australian tree species (Adams et al. 2017). We carried out a series of ecophysiological experiments to identify thresholds for the processes leading to hydraulic failure.

The original goal of our third stream was to use remote sensing to validate SDM projections (i.e. projections identifying in which locations species were likely to have experienced dry stress during the Millennium Drought). This was to build upon work undertaken in other parts of the world where it has been possible to identify large-scale drought mortality events via remote sensing, and develop empirical models to identify climate water balance thresholds (e.g. Anderegg et al. 2015). However, this work could not advance due to a) loss of the chief investigator of this stream and b) discrepancies between the spatial scale of drought mortality and available remotely sensed data. With a collaborator from the US, Professor Chris Williams, we investigated the impact of the Millennium Drought on remotely-sensed indicators of vegetation function, and a paper from this work is currently in review (Jiao et al. in review). However, as the work did not ultimately provide insights into tree mortality, it is not presented in this report. Section 4 presents a short discussion of attempts to monitor tree mortality at landscape scale.

2. Species Distribution Models

Introduction

Our goals for this section were to assess the likely exposure of stands of 47 key NSW tree species to dry stress a) during the Millennium Drought (2001-2009, recognised as the most severe drought on record for southeast Australia, van Dijk et al. (2013)) and b) under scenarios of future climate projected for 2030 and 2070. In doing so, we followed the approach of Aubin et al. (2018) and developed species-specific indices of sensitivity to dry stress. Sensitivity is defined as occurring when a stand experiences moisture balance below the 2.5th percentile of the species’ “hydric envelope” which, in turn, is calculated from the Climate Moisture Index (CMI). This metric characterises moisture balance for a given species at a given location: positive values for CMI indicate an excess of monthly precipitation, relative to monthly potential evapotranspiration, while negative values indicate a moisture deficit. As such, CMI enables stands that likely experience dry stress to be rapidly identified. This approach to assessing sensitivity contrasts with, and complements, mechanistic models (such as those described in Section 3 of this report) which quantify sensitivity using data-intensive models.

Method

Study species:

We identified 47 key canopy tree species common to different forest types in NSW to form the basis of this part of our project (Table 1). Tree species occurrence records from across Australia were obtained from the Atlas of Living Australia (ALA, www.ala.org.au). Records underwent a rigorous cleaning process to remove those that were not georeferenced, had coordinate uncertainty greater than 1000 m, were noted by ALA as spatial/environmental outliers, represented duplicate records, or were cultivated. Records for each species were then overlaid on a 1 km x 1 km raster grid (see Climate Data) and reduced to a single point per species within each cell. We refer to each of these points as a stand.

Table 2.1. 47 canopy tree species commonly found in New South Wales forests, for which exposure to dry stress was assessed. N (Aus) and N (NSW) indicate the number of 1 km x 1 km grid cells containing occurrence records for each species across Australia and NSW, respectively, based on data from the Atlas of Living Australia. For each species, we list the key forest type it is found in, although note that species can also be found in other forest types too: RF = Rainforest, DSF = Dry Sclerophyll Forest, SAW = Semi-arid Woodland, GW = Grassy Woodland, WSF = Wet Sclerophyll Forest, ALP = Alpine.

Species	Veg. Type	N (Aus)	N (NSW)	Species	Veg. Type	N (Aus)	N (NSW)
Antherospermataceae				Myrtaceae (cont.)			
<i>Doryphora sassafras</i>	RF	1,704	1,692	<i>Eucalyptus grandis</i>	WSF	926	757
Casuarinaceae				<i>Eucalyptus largiflorens</i>	SAW	2,146	1,489
<i>Allocasuarina torulosa</i>	DSF	4,966	4,594	<i>Eucalyptus macroryncha</i>	GW	6,759	3,528
<i>Casuarina pauper</i>	SAW	2,852	890	<i>Eucalyptus melliodora</i>	GW	3,961	3,266
Cunoniaceae				<i>Eucalyptus microcorys</i>	WSF	3,860	3,507
<i>Ceratopetalum apetalum</i>	RF	1,606	1,598	<i>Eucalyptus moluccana</i>	DSF	2,762	2,330
Cupressaceae				<i>Eucalyptus obliqua</i>	WSF	9,512	1,387
<i>Callitris glaucophylla</i>	SAW	8,026	6,078	<i>Eucalyptus pauciflora</i>	ALP	3,231	1,990
Fabaceae				<i>Eucalyptus pilularis</i>	WSF	3,650	3,379
<i>Acacia aneura</i>	SAW	4,022	495	<i>Eucalyptus populnea</i>	SAW	2,287	1,875
<i>Acacia harpophylla</i>	SAW	701	316	<i>Eucalyptus racemosa</i>	DSF	2,186	1,971
<i>Acacia melanoxylon</i>	RF	16,515	4,450	<i>Eucalyptus rossii</i>	DSF	1,600	1,600
<i>Acacia melvillei</i>	SAW	477	286	<i>Eucalyptus saligna</i>	WSF	2,798	2,697
Myrtaceae				<i>Eucalyptus sideroxylon</i>	DSF	1,034	975
<i>Angophora costata</i>	DSF	2,784	2,760	<i>Eucalyptus teretecornis</i>	DSF	5,395	4,124
<i>Angophora floribunda</i>	GW	6,412	6,148	<i>Eucalyptus viminalis</i>	WSF	13,987	2,631
<i>Corymbia gummifera</i>	DSF	3,827	3,749	<i>Syncarpia glomulifera</i>	WSF	4,568	4,252
<i>Eucalyptus albens</i>	DSF	4,361	3,876	<i>Syzygium smithii</i>	RF	270	109
<i>Eucalyptus blakelyi</i>	GW	2,971	2,844	<i>Tristaniopsis laurina</i>	RF	1,726	1,312
<i>Eucalyptus bridgesiana</i>	GW	3,372	2,586	Nothofagaceae			
<i>Eucalyptus camaldulensis</i>	SAW	14,433	3,414	<i>Nothofagus moorei</i>	RF	271	271
<i>Eucalyptus coolabah</i>	SAW	2,930	1,489	Pittosporaceae			
<i>Eucalyptus crebra</i>	DSF	6,051	3,821	<i>Pittosporum undulatum</i>	RF	7,658	5,387
<i>Eucalyptus cypellocarpa</i>	WSF	5,039	1,876	Proteaceae			
<i>Eucalyptus dalrympleana</i>	WSF	3,015	2,248	<i>Banksia serrata</i>	DSF	4,458	3,196
<i>Eucalyptus deanei</i>	WSF	846	839	<i>Hakea leucoptera</i>	SAW	1,769	462
<i>Eucalyptus delegatensis</i>	WSF	4,533	370	Sapindaceae			
<i>Eucalyptus dumosa</i>	SAW	4,526	1,338	<i>Alectryon oleifolius</i>	SAW	5,071	2,091

Climate data and calculation of Hydric Envelope:

We obtained monthly precipitation (P) and potential evapotranspiration (PET) data from two key sources: a) eMAST (Ecosystem Modelling and Scaling Infrastructure Facility; www.emast.org.au), for the baseline

period (1970-2000) and Millennium Drought (2001-2009), and b) NSW and ACT Regional Climate Modelling project (NARClIM) (Evans et al. 2014; Hutchinson & Xu 2015) for the near-future (2020-2039) and distant future (2060-2079). NARClIM consists of climate surfaces projected by four Global Climate Models (GCMs) (Table 2.2) that were dynamically downscaled using three configurations of the Weather and Research Forecasting (WRF version 3; Skamarock et al. 2008) Regional Climate Model (RCM). This resulted in 12 climate scenarios that encompass a range of equally plausible climate futures for south-eastern Australia. Each GCM is therefore represented by three scenarios, and to improve interpretability we refer to the four GCMs as simulating Warmer/wetter, Hotter/Little change in precipitation, Hotter/wetter and Warmer/drier futures, with respect to baseline conditions.

All climate data were transformed to the Australian Albers Equal-Area Conic projection (EPSG: 3577) at 1 km x 1 km resolution. We then calculated the Climate Moisture Index (CMI) for each time period and climate scenario, using the sum of P minus PET for the Austral summer, averaged across all years within each time frame.

Table 2.2. NARClIM scenarios included in this study. GCMs assumed the SRES A2 emissions scenario (Nakicenovic et al. 2000).

Climate Future	GCM	Represents a future that is:
Warmer/Wetter	MIROC3.2(medres)	Warmer and wetter than present, particularly in NE NSW, although alpine regions are projected to become drier.
Hotter/Little Change in Precipitation	ECHAM5/MPI-OM	Has the greatest increase in temperature of the four scenarios. Precipitation trend varies across the state (slightly wetter in the NE and coastal regions, slightly drier elsewhere).
Hotter/Wetter	CCCMA CGCM3.1(T47)	Warmer than MIROC, and wetter across most of the state, although areas in NW and SE of the state may be slightly drier.
Warmer/Drier	CSIRO-Mk3.0	Warmer than present, and the driest of the four models.

To calculate the breadth of each species' hydric envelope (i.e. the range of values for CMI across all stands), we overlaid the species' set of occurrence records (i.e. stands) onto the baseline (pre-drought) CMI, and quantified the minimum, maximum, and 2.5th percentile values for CMI. We categorised any stand with a CMI value between the species' minimum and 2.5th percentile as dry stressed. Next, we overlaid species' occurrence records with CMI layers for the Millennium Drought and each of 12 NARClIM near- and distant-future scenarios. Values for CMI under each of these scenarios were obtained. Then, using the 2.5th percentile threshold quantified from the baseline CMI layer, we identified which stands were likely to have been exposed to dry stress during the Millennium Drought or may be exposed to dry stress in the future. To assess consistency across the 12 future scenarios, we grouped results according to the GCM that the climate scenario was derived from. For each species we identified stands that are projected to be dry stressed under a) all three of the RCMs for a given GCM and b) all four GCMs (i.e. all 12 RCMs), in both future time periods. Finally, for each time period, we combined maps for all species to identify key geographic regions of stress. All analyses were undertaken using the software R version 3.1.2 (R Development Core Team 2014).

Results

Pre-drought and Millennium Drought

The minimum and maximum values of each species' hydric envelope, and its 2.5th percentile stress threshold is given in Appendix 2. The number of stands within NSW/ACT exposed to dry stress in the pre-drought period (1970-2000) averaged 41 ± 38 (SD), ranging from 0 for eight of the species to 147 for two species (*Eucalyptus macroryncha*, *Pittosporum undulatum*) (Appendix 3). During the Millennium Drought, an average of 247 ± 237 stands (11.9% \pm 10.5%) in NSW/ACT stands experienced dry stress. Four species (*Acacia aneura*, *Eucalyptus coolabah*, *Eucalyptus crebra*, and *Hakea leucoptera*) were unlikely to have any NSW/ACT stands below the 2.5th percentile of their respective hydric envelope during the drought. In contrast, between 27-47% of stands for *Eucalyptus sideroxylon*, *Eucalyptus cypellocarpa*, *Acacia harpophylla*, *Eucalyptus bridgesiana*, and *Eucalyptus dumosa*, were likely dry stressed. For each species, maps of stands that likely experienced dry stress in the periods pre- and during the millennium drought are in Appendix 4.

In each grid cell, we tallied the number of species with stands (Figure 2.1), and the number of stands exposed to dry stress in the pre-drought and Millennium Drought periods. Higher numbers of the 47 species are found in the Sydney Basin and North Coast regions. While species within the Sydney Basin, and South Coast regions were exposed to dry stress during the millennium drought, few in the North Coast region were.

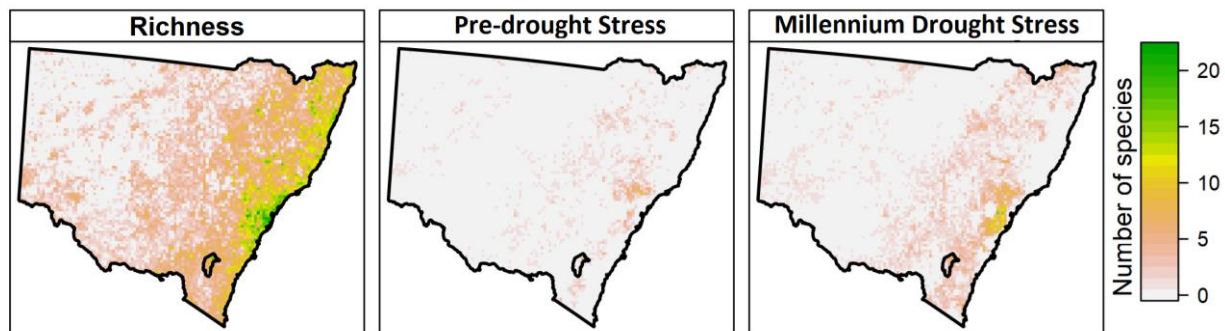


Figure 2.1. Dry stress among stands of 47 NSW/ACT tree species. The Richness map indicates the number of species ($n = 47$) with stands present in 1 km x 1 km grid cells. The Pre-drought Stress and Millennium Drought Stress maps indicate the number of species ($n = 47$) with stands exposed to dry stress (i.e., Climate Moisture Index less than the species' pre-drought 2.5th percentile) in the pre-drought period (1970-2000) and during the Millennium Drought (2001-2009).

Future scenarios

For 2030 and 2070, we assessed dry stress under the 12 NARClIM scenarios, grouping results according to the GCM that the scenario was derived from (Appendix 3). As mentioned previously, to improve

interpretability we refer to these scenarios as Warmer/wetter, Hotter/Little change in precipitation, Hotter/wetter and Warmer/drier, with respect to baseline conditions (Table 2.1). Unsurprisingly, fewer stands are projected to experience dry stress under the two wetter scenarios (2030: Hotter/wetter average 12 ± 17 (SD) stands ($0.6\% \pm 0.7\%$); Warmer/wetter average 10 stands ± 16 ($0.5\% \pm 1.0\%$) (Figure 2.2). More stands are projected to experience stress under CSIRO’s Warmer/drier scenario (2030: average 108 ± 96 ($5.3\% \pm 4.5\%$)). Across the 47 species, this ranges from 0% of stands for seven species (*Acacia aneura*, *Eucalyptus coolabah*, *Eucalyptus crebra*, *Hakea leucoptera*, *Eucalyptus tereticornis*, *Eucalyptus camaldulensis*, *Alectryon oleifolius*) to > 10% for *Eucalyptus deanei*, *Eucalyptus dumosa* and *Acacia harpophylla*. By 2070, average results under this scenario remain similar to 2030.

For each species, we also calculated the percentage of NSW/ACT stands projected to be exposed to drought stress irrespective of the future scenario that occurs. By 2030, this ranges between 0-3.0% of stands (average $0.4\% \pm 0.5\%$), increasing slightly to a maximum of 3.0% by 2070 (average $0.2\% \pm 0.5\%$).

Finally, we developed maps illustrating the number of species with stands projected to experience dry stress under each future scenario within each grid cell (Figure 2.3).

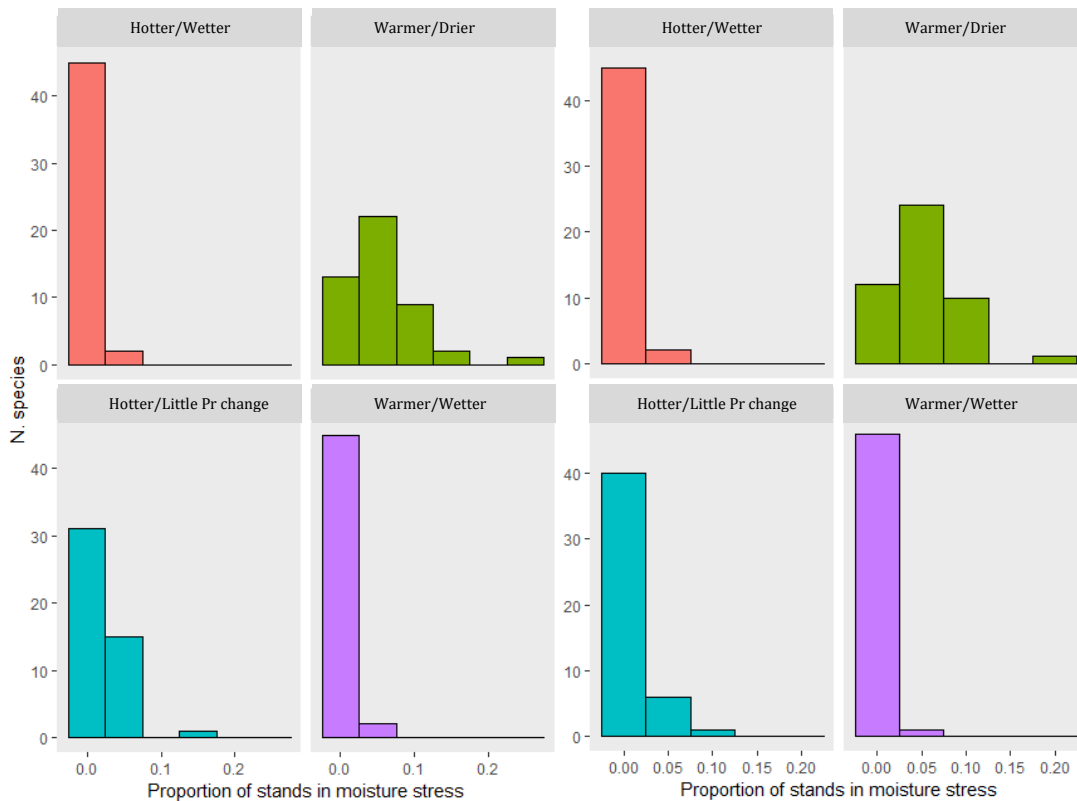


Figure 2.2. Proportion of stands for 47 NSW/ACT tree species projected to experience dry stress over the period 2020-2039 (left) and 2070 (right), under four climate change scenarios (CCCMA = Hotter/Wetter; CSIRO = Warmer/Drier; ECHAM = Hotter/Little precipitation change; MIROC = Warmer/Wetter).

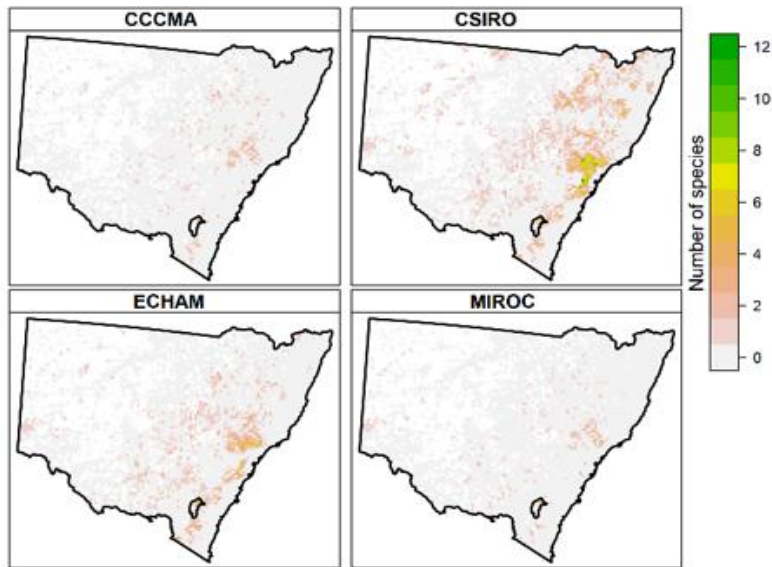


Figure 2.3. Number of species with stands exposed to dry stress under four scenarios for the period 2020-2039 (CCCMA = Hotter/Wetter; CSIRO = Warmer/Drier; ECHAM = Hotter/Little precipitation change; MIROC = Warmer/Wetter).

Discussion

This study demonstrates a straightforward approach to quantify the hydric envelopes of 47 key tree species, and highlights stands that were likely to have experienced dry stress during the Millennium Drought (MD). Our results indicate that it was primarily stands on the western margin of species' ranges that were most exposed to dry stress during the MD. Our approach provides a rapid assessment of the relative exposure of stands to dry stress under future climate scenarios for south-eastern Australia (NARClIM). The resulting maps may be useful for management of species over the near future, with multi-species maps helping to identify regions where several species may be at risk of dry stress over the same time-frame.

However, we emphasise several caveats. Firstly, as it is based on species' occurrences, our approach is correlative only and will be influenced by the extent to which species geographic ranges are limited by climatic variables. As such, this study would be strengthened substantially by information on declines in productivity or mortality during the MD, as well as comparisons with mechanistic models currently being developed. Secondly, while our measure of dry stress (i.e. < 2.5th percentile of the species' hydric envelope during the baseline period) has some theoretical basis and has been demonstrated elsewhere previously (Aubin et al. 2018), the choice of threshold is somewhat arbitrary and is yet to be compared to ecophysiological experiments. The mismatch between the length of time periods that we considered may also be relevant. Data describing future periods represented a 20-year span, compared to the ~30-year span of the pre-drought period and 9-year span of the MD period. Since the mean CMI of shorter periods

is more sensitive to interannual variation, the accuracy of this variable may not be consistent across periods. However, the CMIP3 climate models upon which the future projections were based are relevant to south-eastern Australia, and NARClIM remains the most appropriate future climate data for this region. Nevertheless, future work could extend our analysis by using updated climate projections as such data become available.

3. Ecophysiological Experiments

Introduction

The goal of this stream of the project was to develop our physiological understanding of the mechanisms leading to tree mortality during drought, in order to be able to predict the thresholds above which mortality risk increases.

There are several different mechanisms that can lead to tree death during drought (McDowell et al. 2008). Hydraulic failure occurs when the plant's xylem cavitates under stress, breaking the water supply column from the roots to the leaves. Carbon starvation occurs when stomata shut to prevent water loss, but this also prevents photosynthesis, depriving the plants of the carbohydrate supply needed for respiration. Long-term drought stress can also weaken a plant's defense mechanisms, rendering them susceptible to pests and pathogens.

Adams et al. (2017) conducted a review of drought mortality studies and found that, of the two physiological mechanisms, hydraulic failure is the most prevalent. In all studies they reviewed, there was a loss of hydraulic function leading to death, whereas only a few studies showed evidence of carbon starvation, and these were mostly of gymnosperms (non-flowering plants). Biotic factors are also implicated in many Australian dieback events associated with drought, but these are considerably more challenging to study experimentally, and are also likely to co-occur with hydraulic failure. Hence, we focused our experimental studies on hydraulic thresholds.

There are two major phases in the progression to drought death by hydraulic failure: the phase of stomatal closure, and the phase of desiccation (Figure 3.1) (Choat et al. 2018). During the initial phase of drought, plants close their stomata to control the rate of water loss. Most recent studies indicate that stomata in trees close before reaching the threshold xylem water potential at which significant cavitation is initiated. In the second phase, after the point of stomatal closure, plants continue to lose water at a slow rate via cuticular conductance, stomatal leakiness and evaporation from other tissues such as bark. As water is lost, the xylem water potential continues to fall, ultimately reaching a critical threshold at which cavitation spreads throughout the plant, causing whole-plant death.

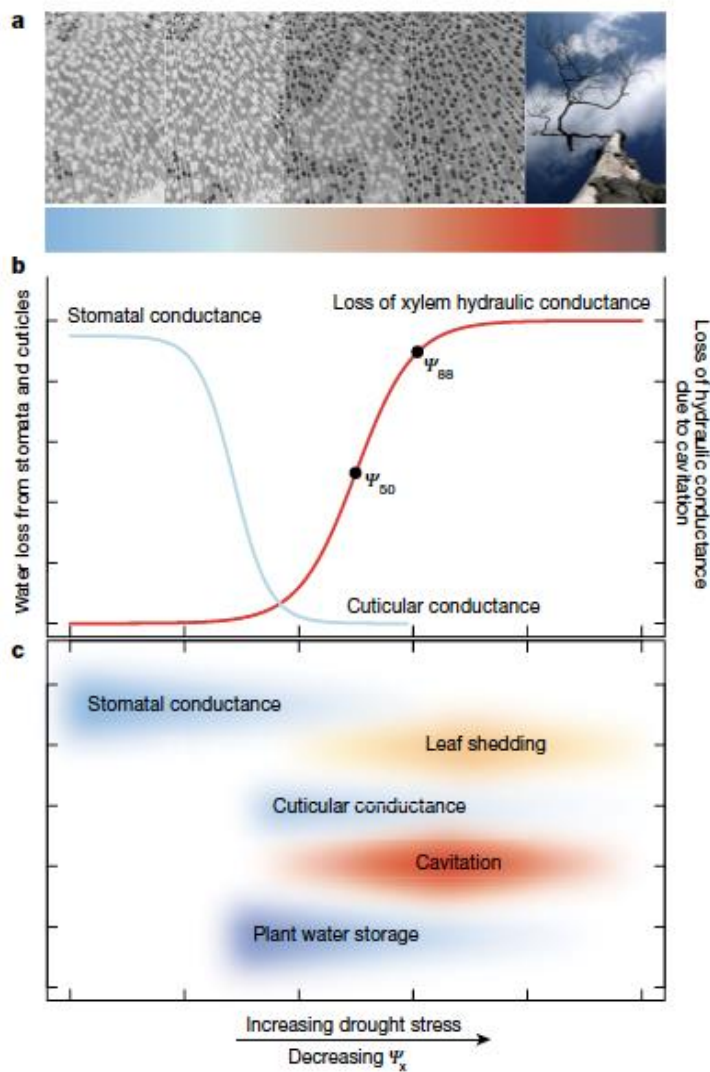


Figure 3.1 Phases of drought response in plants. *a*, time series of transverse slices through the xylem tissue obtained by X-ray microtomography show spread of gas emboli through the xylem with increasing drought stress (left to right). In each slice, water filled vessels are seen as bright circles while vessels contain gas emboli are black. During severe drought, almost all vessels become gas filled leading to whole plant mortality *b*, During the first phase, stomata close to limit water loss and delay the decrease in xylem water potential (blue line). After stomata close, water continues to be lost at a much lower rate via cuticular conductance. At a critical threshold, cavitation increases rapidly and gas emboli spread throughout the xylem (red line). Increasing levels of embolism are shown as the proportional loss of xylem hydraulic conductance. ‘Vulnerability curve’ analysis translates the physics of cavitation to a quantification of species susceptibility to cavitation during the water stress exposure. These mortality thresholds have been found to correspond to between 50% (ψ_{50}) and 88% (ψ_{88}) loss of hydraulic function in conifers and angiosperms, respectively. *c*, A general scheme for the magnitude and timing of response processes with increasing drought stress. [Taken from Choat et al. 2018]

We carried out a series of experiments targeting these different phases. The first major experiment focused on the first phase, and measured traits describing the processes of stomatal closure and loss of hydraulic conductance in 14 NSW species. The second major experiment focused on the second phase, and measured traits enabling us to predict the rate of plant desiccation following stomatal closure. Additional, smaller studies addressed (i) intraspecific trait variability, allowing us to examine the adaptive capacity of species to drought; and (ii) recovery of xylem function following drought dieback. Each of these studies has provided important scientific insights into plant function during drought that will ultimately enable us to develop ecophysiology-based forecasts of drought mortality.

Experiment 1: Stomatal and hydraulic traits

The goal of the first major experiment was to quantify the key traits describing stomatal and hydraulic function in tree species that represent NSW vegetation types. Full details of the experimental protocol and results from Experiment 1 are given in Li et al. (2018a).

Twelve dominant tree species, representing five major woody vegetation types in NSW were used in Experiment 1. Vegetation types and species within each vegetation type are listed in Table 3.1. Species vary markedly in climate-of-origin, with mean annual temperature (MAT) spanning from 10 °C to 20.5 °C, and mean annual precipitation (MAP) ranging from 188 mm to 1125 mm. Aridity index (AI), calculated as the ratio of MAP and potential evaporation (PET), varies between 0.1 (most arid) for *Acacia aneura* and 1.1 (least arid) for *Eucalyptus viminalis*.

Table 3.1: Experimental species

Species	Abbreviation	Vegetation type	MAT	MAP	AI
<i>Acmena smithii</i>	Asm	Rainforest	14.9	837.4	0.9
<i>Eucalyptus grandis</i>	Egr	Wet sclerophyll forest	18.6	1124.5	0.9
<i>Eucalyptus viminalis</i>	Evi		10	751.5	1.1
<i>Angophora costata</i>	Aco	Dry sclerophyll forest	17.2	877.8	0.8
<i>Corymbia gummifera</i>	Cgu		16.8	880.3	0.8
<i>Eucalyptus sideroxylon</i>	Esi		16.4	478.1	0.4
<i>Eucalyptus blakelyi</i>	Ebl	Grass woodland	15.1	550.2	0.5
<i>Eucalyptus macrorhyncha</i>	Ema		13.8	546.5	0.7
<i>Eucalyptus melliodora</i>	Eme		14.7	526.1	0.5
<i>Acacia aneura</i>	Aan	Semi-arid woodland	20.5	188.2	0.1
<i>Eucalyptus largiflorens</i>	Ela		17.4	250.2	0.2
<i>Eucalyptus populnea</i>	Epo		18.8	370.6	0.3

For each species, four individuals were assigned to a well-watered treatment, and were watered daily over the experimental period. The remaining individuals (20 plants) were assigned to a drought treatment. The unbalanced allocation of individuals to treatments enabled drought plants to be destructively

sampled across a range of xylem water potentials during soil drying. The drought treatment was implemented by withholding irrigation during two drought cycles. In the first drought cycle, plants were dried until leaves were visually wilting, which occurred in one to two weeks depending on weather conditions and species drought sensitivity. Thereafter, irrigation was resumed and plants were watered daily for ten days to allow full recovery. In the second drought cycle, irrigation was discontinued and plants were stressed until the end of experiment.

Table 3.2 summarises the measurements made during the course of the experiment and their significance for plant function. The measurements include traits that describe the rate of stomatal closure during soil drying (P_{gs50}, P_{gs90}); the rate at which xylem embolises (P₁₂, P₅₀, P₈₈); standard plant functional traits characterising the species (SLA, WD); and traits describing the carbon uptake capacity and growth rate of the plants (A_{max}, VIGR).

Table 3.2: Trait measured in Experiment 1 and their significance for plant carbon and hydraulic strategies

Traits	Units	Definition	Significance
$\Psi_{\text{leaf}}, \Psi_{\text{stem}}$	MPa	Leaf and stem water potential	Potential energy of water; indicators of organ water status
P ₁₂	MPa	Ψ_{stem} at 12% loss of conductivity	Inception of stem embolism; closely linked to leaf gas exchange
P ₅₀	MPa	Ψ_{stem} at 50% loss of conductivity	Index of hydraulic safety and drought tolerance across species
P ₈₈	MPa	Ψ_{stem} at 88% loss of conductivity	Hypothetical maximum water stress level in angiosperms, beyond which recovery is impossible
K _s	kg m ⁻¹ s ⁻¹ MPa ⁻¹	Water flow per unit conduit area at given time and pressure gradient	Water transport capacity of stem; index of hydraulic efficiency and may trade off with hydraulic safety
P _{gs50}	MPa	Ψ_{leaf} at 50% of maximum stomatal conductance	Early decline of stomatal conductance; proxy of Ψ_{leaf} at which stomata initiate closure
P _{gs90}	MPa	Ψ_{leaf} at 10% of maximum stomatal conductance	Maximum water stress while still maintaining photosynthesis; proxy of stomatal closure
TLP	MPa	Bulk leaf water potential at which turgor pressure is zero	Ψ_{leaf} when leaf loses turgor and wilts, while leaf becomes physiologically dysfunctional
C _{branch}	RWC MPa ⁻¹	Amount of releasable water of living cells as xylem tension increases	Total releasable water following the reduction of plant water potential, which may facilitate recovery from embolism

HSM	MPa	Hydraulic safety margin, defined as difference between P_{gs90} and P_{50}	HSM integrating leaf and stem hydraulics, reflecting the coordination between different organs and putatively linked to drought resistance
SLA	$m^2 kg^{-1}$	Ratio of leaf area to dry mass	Leaf area produced by given biomass investment; may affect leaf carbon assimilation and plant drought tolerance
A_{max}	$\mu mol m^{-2} s^{-1}$	Maximum carbon assimilation rate under well-watered conditions	Index of leaf photosynthetic capacity
g_{smax}	$mol m^{-2} s^{-1}$	Maximum stomatal conductance under well-watered conditions	Pivotal trait bridging carbon and water exchange
VIGR	$cm^3 day^{-1}$	Stem volume index growth rate	Surrogate of plant growth rate
WD	$g cm^3$	Sapwood density	Highly integrative trait of wood anatomical features

The key result from Experiment 1 was that the stomatal and hydraulic behaviour of each species were closely co-ordinated, and could be predicted from the climate of origin of the species. We found that for each species, stomatal closure occurred at the onset of xylem embolism, showing that all species regulate their stomatal behaviour to prevent embolism. The onset of xylem embolism was strongly correlated with the mean annual precipitation in the climate of origin, demonstrating strong adaptation of both stomatal and hydraulic behaviour to environment.

The relative rates of stomatal closure and loss of xylem conductivity are shown for each species in Figure 3.2. The species are arrayed by climate of origin, progressing from rainforest (*A. smithii*) to semi-arid species (*E. populnea*). The blue lines mark the point of stomatal closure (P_{gs90}) while the red lines mark the point at which 50% of xylem conductivity is lost (P_{50}). As can be seen in the Figure, both points shift to the right as we move from mesic to xeric species, showing the co-ordination between these traits and their adaptation to the environment.

These points are further demonstrated in Figures 3.3 and 3.4. Figure 3.3 demonstrates that, across species, the point of stomatal closure (P_{gs90}) coincides with the point of onset of xylem embolism (P_{12}). Figure 3.4 shows the very strong relationships seen between both the point of stomatal closure (P_{gs90}) and the rate of loss of hydraulic conductivity (P_{50}) with the mean annual precipitation and the aridity index averaged across each species' native distribution.

The results from Experiment 1 are important because they help us to identify how key thresholds during drought vary in trees across the landscape.

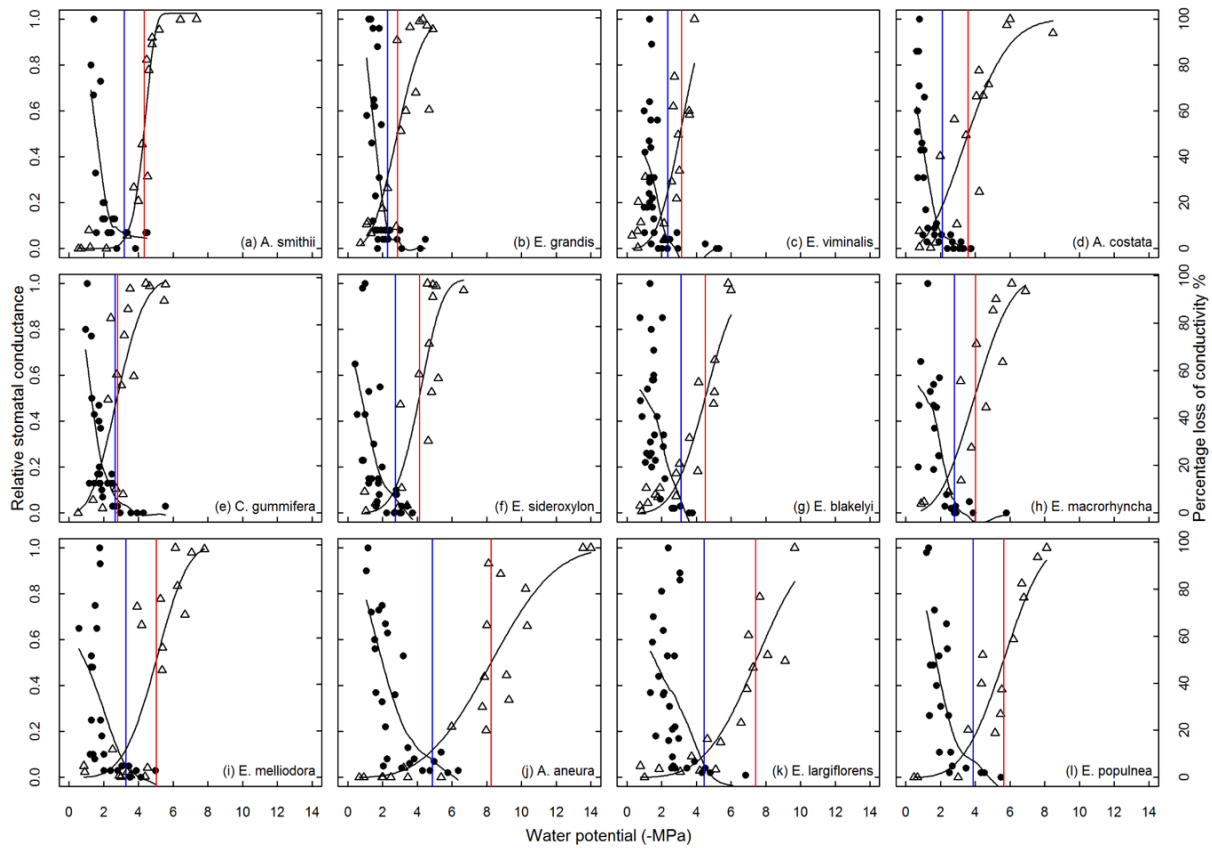


Figure 3.2 Percentage loss of xylem conductivity (PLC, open triangle) and relative leaf stomatal conductance (closed circle) response to water potential of twelve woody species. Red and blue vertical lines indicate xylem water potential inducing 50% loss of conductivity (P_{50}) and leaf water potential at 90% stomatal closure (P_{gs90}), respectively; distance between lines denotes the hydraulic safety margin (HSM). [From Li et al. 2018a]

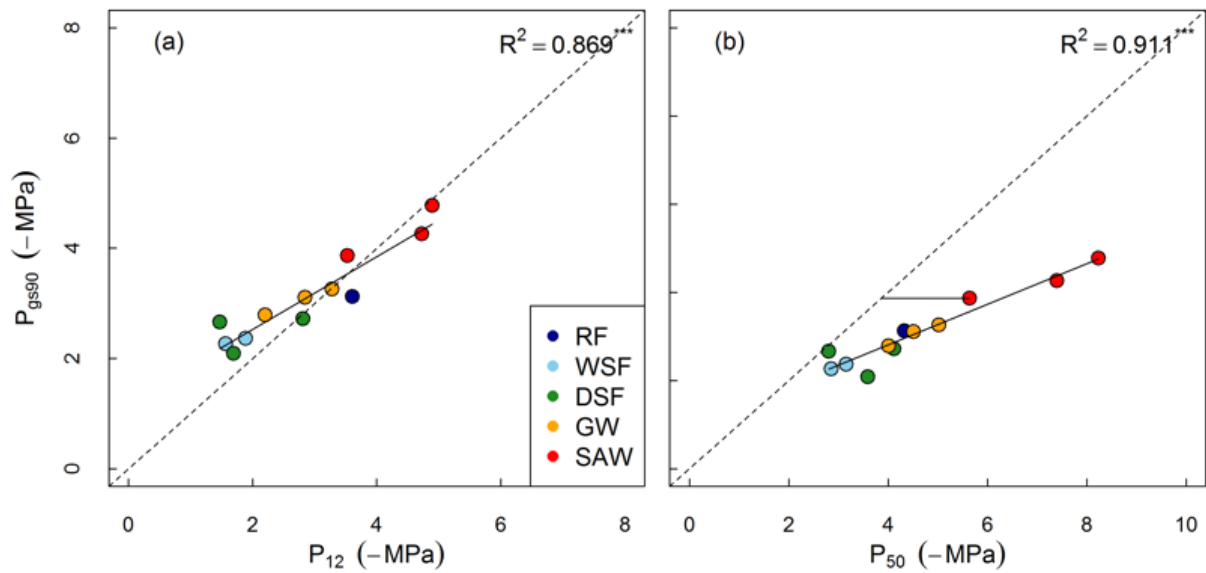


Figure 3.3 The relationship between xylem water potential at 90% stomatal closure (P_{gs90}) and xylem water potential at the inception of xylem cavitation (P_{12} ; Figure 2a), and 50% loss of conductivity (P_{50} ; Figure 2b). Horizontal line in Figure 2b indicates HSM. Error bars indicate standard error of mean. Adjusted R^2 of linear regressions (solid lines) are provided. Statistical significance is indicated by asterisk (***, $P < 0.001$; **, $P < 0.01$; *, $P < 0.05$; ns, not significant). Five vegetation types (rainforest (RF), wet sclerophyll forest (WSF), dry sclerophyll forest (DSF), grass woodland (GW), and semi-arid woodland (SAW)) are represented by different colours. Dashed lines indicate 1:1 relationship. [From Li et al. 2018a]

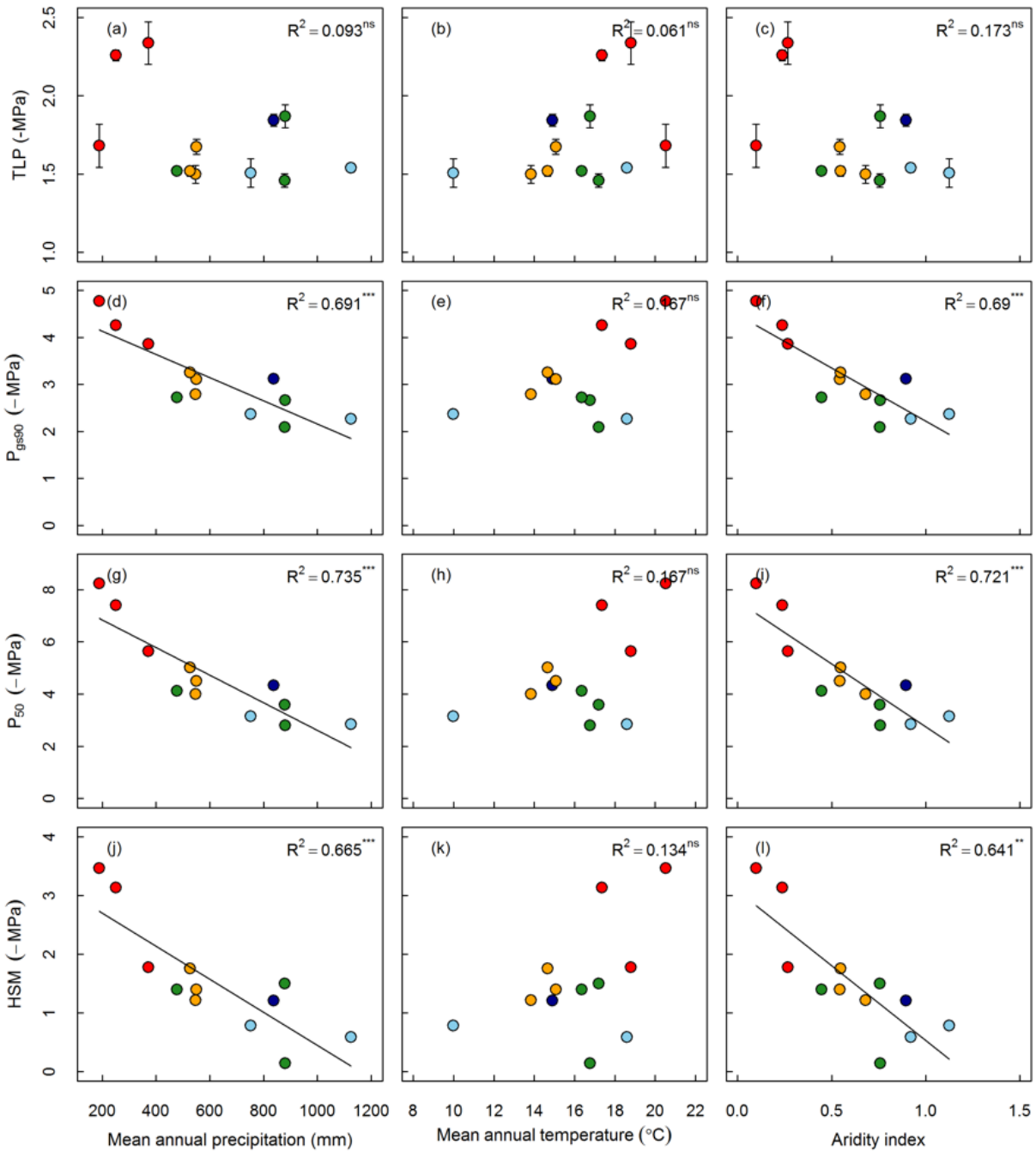


Figure 3.4 Effect of site water availability, characterized by mean annual precipitation (MAP) and aridity index (AI), and mean annual temperature (MAT) on leaf turgor loss point (TLP, Figure 7a-c), water potential at 90% stomatal closure (P_{gs90} , Figure 7d-f), xylem cavitation resistance (P_{50} , Figure 7g-i) and hydraulic safety margin (HSM, Figure 7j-l). Adjusted R^2 of linear regressions are shown for each correlation, but regression lines are only drawn for statistically significant cases. Statistical significance is indicated by asterisk (***, $P < 0.001$; **, $P < 0.01$; *, $P < 0.05$; ns, not significant). [From Li et al. 2018a]

Experiment 2: Desiccation time

The goal of the second major experiment was to measure additional traits describing the progression of the second, desiccation phase of drought, and to use these results to predict time to mortality following stomatal closure, using the model developed by Blackman et al. (2016). The experimental design is described in Li et al. (2019b). The results are presented in Blackman et al. (in review).

The model presented by Blackman et al. (2016) to predict desiccation time is:

$$t_{\text{crit}} = \frac{(\theta_0 - C \cdot \Psi_{\text{crit}}) V_w}{A_L g_0 D}$$

Where t_{crit} is the time taken for trees to desiccate from stomatal closure to lethal levels of water stress (s), θ_0 is the relative water content (RWC, g g^{-1}) at stomatal closure; C is the branch capacitance (mmol Mpa^{-1}); Ψ_{crit} is the critical stem water potential thought to cause mortality (in this study with angiosperms, we used the water potential at 88% loss of stem conductivity); V_w = the total amount of water in the plant (g); A_L = total leaf area (m^2); g_0 = the minimum leaf conductance ($\text{g m}^{-2}\text{s}^{-1}$); and D = vapour pressure deficit (mol mol^{-1}). We extended this model to incorporate leaf shedding.

Eight species of *Eucalyptus* were chosen to test whether plant desiccation times were predictable. For this experiment, 15-20 plants of each species were grown in 75L grow bags in the WSU polytunnel facility. Plants were grown for 7 months under well-water conditions, then drought-hardened by withholding water until visual signs of leaf wilt were present, after which they were rewatered and allowed to recover for four-six days. At the end of this recovery period six plants per species were designated for a range of trait measurements needed for the desiccation model, including saturated plant water content, branch capacitance, minimum leaf conductance and leaf hydraulic vulnerability. Water was withheld from the remaining plants per species (n = between 6 and 12), after which they were allowed to use up available soil water and then desiccate to critical levels of water stress.

During the dry-down treatment, each individual was checked daily for signs of leaf death. Leaves were deemed to be dead (i.e. completely desiccated) when they became paler in colour and 'crispy' to touch. For most species, leaf death started in the oldest leaves at the base of the main stem and then progressed toward the newer leaves in the upper canopy.

The point in time at which individuals of each species dehydrated to their respective water potentials at stomatal closure ($g_s P_{90}$) and critical point of xylem embolism (stem P_{88}) was interpolated from the relationship between pre-dawn water potential and accumulated VPD measured over the course of each dry-down experiment. The average time span (i.e., VPD hrs) between the water potential at stomatal closure and stem P_{88} was determined for each species from a linear mixed model (with individual input as a random factor) fitted to the $\Psi \sim \text{VPD hrs}$ data. The resultant plant desiccation time observed for each species is referred to as $t_{\text{crit_obs}}$.

The data from this experiment are shown in Figure 3.5, which illustrates the progression of stem water potential to the critical value, and the concurrent rate of leaf death.

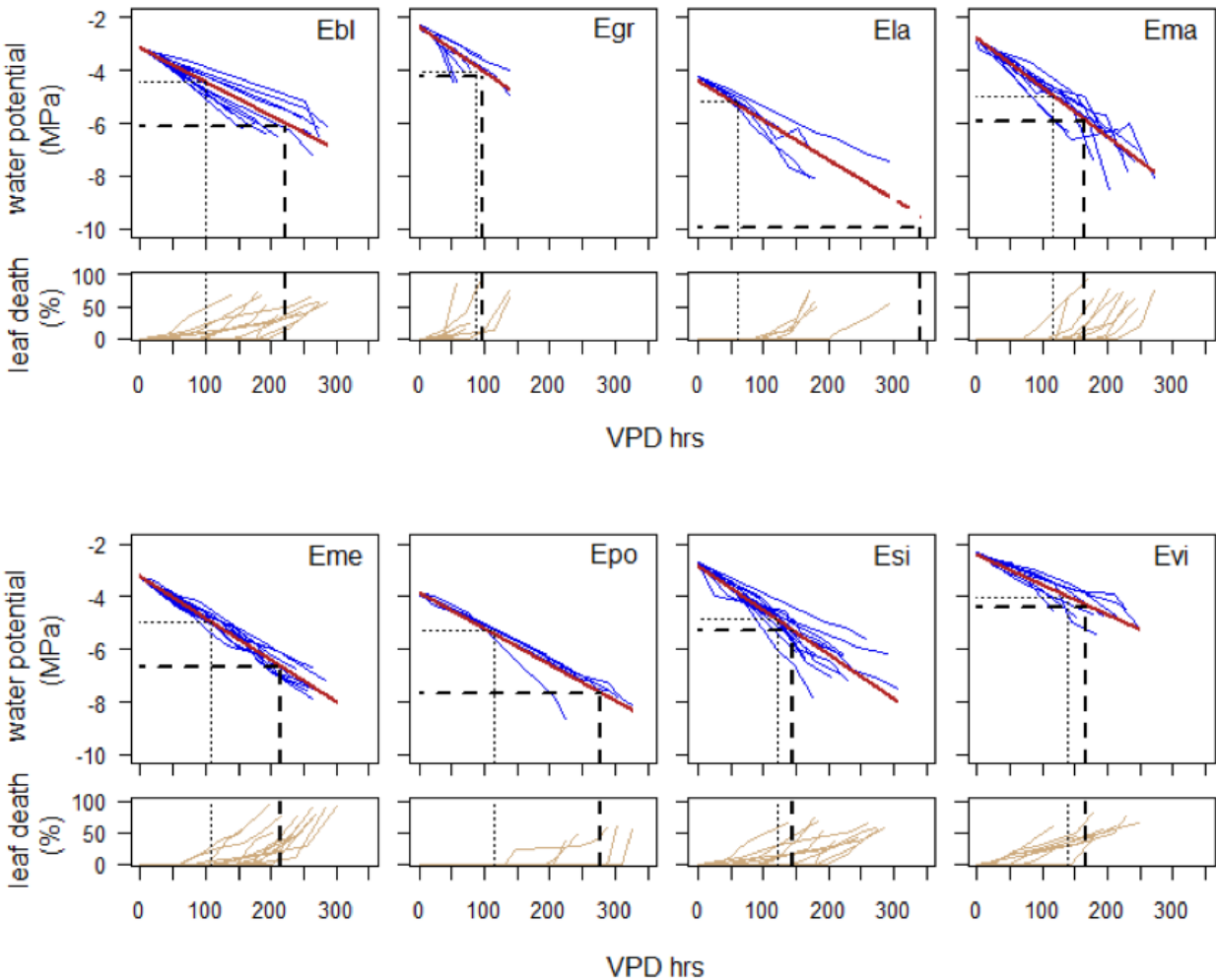


Figure 3.5 The response of water potential (Mpa, large panels) and leaf death (% of total leaf area, small panels) observed for individuals of each species over time (VPD hrs) during plant desiccation from the point of stomatal closure to when plants were harvested (ca.50-70% leaf death). The regression line (red) was determined for each species using a mixed-effects model with individual input as random effects. In each panel, the vertical dashed line represents the time to stem P_{88} (horizontal dashed line), while the vertical dotted line represents the time to leaf P_{88} (horizontal dotted line). Species are as follows: Ebl, *Eucalyptus blakelyi*; Egr, *E. grandis*; Ela, *E. largiflorens*; Ema, *E. macrorhyncha*; Eme, *E. melliodora*; Epo, *E. populnea*; Esi, *E. sideroxylon*; Evi, *E. viminalis* [Taken from Blackman et al., in review]

The key result from this experiment was that desiccation time could be predicted extremely well for each species. As shown in Figure 3.6, when we applied the model proposed by Blackman et al. (2016) we could capture the variation in desiccation time across species, but the model under-predicted the desiccation time. We hypothesised that leaf shedding by the plants was enabling them to extend the

desiccation time by reducing the amount of leaf area through which stored water could be lost. We extended the Blackman et al. (2016) model to incorporate leaf shedding and found that desiccation time could be very accurately predicted from the revised model.

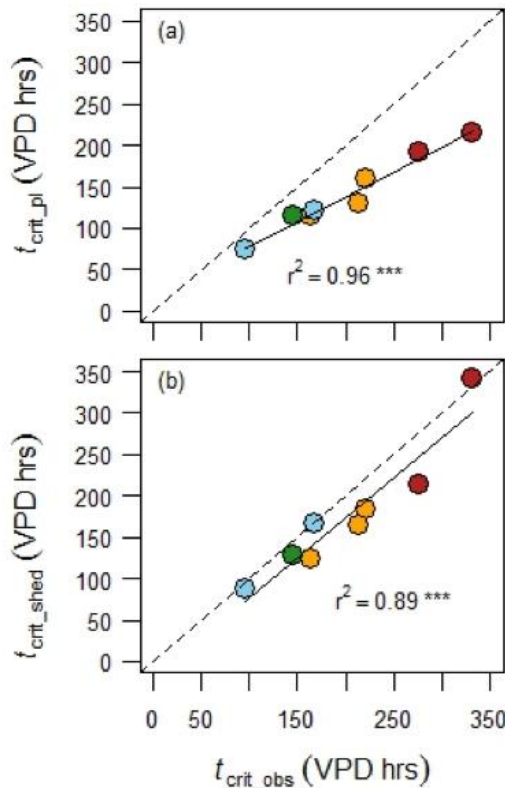


Figure 3.6 Observed (t_{crit_obs}) vs modelled desiccation times recorded for each species. Modelled plant desiccation times were calculated using whole plant traits with a fixed leaf area (t_{crit_pl} ; plot a) and whole plant traits combined with leaf shedding (t_{crit_shed} ; plot b). Colours indicate vegetation type: light blue = WSF, green = DSF, orange = GW, red = SAW (see Table 3.1). [Taken from Blackman et al. in prep]

The results from Experiment 2 are an important scientific advance because they help us to predict the time to mortality once the point of stomatal closure has been passed.

Additional experiments

During the course of the project, opportunities arose for additional experiments to examine targeted ecophysiological questions relating to the progression of drought mortality. Here we provide an overview of the key findings from these experiments. Full details of these experiments can be found in the papers by Li et al. (2018b, 2019b).

Firstly, we took advantage of a natural dieback event occurring in the Blue Mountains in autumn-winter 2017, to study recovery of *Eucalyptus piperita* from dieback (Li et al. 2018b). We aimed to test whether hydraulic failure could be implicated as the mechanism causing the dieback. We also aimed to test the ability of this species to repair xylem embolism following hydraulic failure. It has been proposed that embolism refilling occurs once water stress is alleviated and plant water status is restored, and that for

some plant species a cycle of xylem embolism-refilling occurs on a daily basis (Meinzer and McCulloh 2013; Ogasa et al. 2013). However, the refilling hypothesis is not supported by other studies examining xylem embolism during drought and recovery cycles (Charrier et al. 2016; Choat et al. 2015), suggesting that embolism refilling may not be a universal strategy, especially in trees.

One month after drought-induced leaf and branch dieback was observed in field populations of *E. piperita* in the Blue Mountains, we measured the level of native stem embolism and characterised the extent of leaf death in co-occurring dieback and healthy (non-dieback) trees. We found that canopy dieback-affected trees showed significantly higher levels of native embolism (26%) in tertiary order branchlets than healthy trees (11%). Furthermore, there was a significant positive correlation ($R^2 = 0.51$) between the level of leaf death and the level of native embolism recorded in branchlets from dieback-affected trees. The results of this study confirm that hydraulic failure was the primary mechanism of leaf and branch dieback in response to a natural drought event in the field. It also suggests that post-drought embolism refilling is minimal or absent in this species of eucalypt. This result indicates that restoring post-drought hydraulic function may primarily depend on new xylem growth.

Secondly, we investigated intra-specific variability in drought tolerance traits (Li et al., 2019b). Our main experiments aimed to evaluate these traits at a species level, but it is unclear whether there is significant intra-specific variability in these traits that would enable populations at the drier edge of the distribution to survive more severe droughts. The target species for this study was *Banksia serrata*. We were readily able to access populations from the extremes of this species' distribution. Plant materials were collected from three sites characterized by contrasting climate (Patonga: Warm-Wet, Agnes Banks: Warm-Dry, Mount Banks: Cold-Wet) (Figure 3.7).

Vulnerability to embolism in leaf and stem, defined by the water potential inducing 50% and 88% loss of conductivity (P_{50} and P_{88} , respectively) did not differ across sites. Overall, distinct site water availability did not incur substantial differentiation in hydraulic traits, and the safety-efficiency trade-off was absent in this species. These results suggest that plants growing in the drier sites will be prone to drought risk and indeed, we have seen significant mortality of this species in more exposed sites in the Blue Mountains during the 2018 drought.

Development of process-based model

The experimental research carried out in this project is being used to develop a process-based model that aims to predict drought mortality risk from ecophysiological principles. The model has been implemented in CABLE (the Community Atmosphere Biosphere Land Exchange model, <http://www.cawcr.gov.au/research/cable/>) but at the time of writing is still undergoing testing against experimental data and observations. Output from a simplified version of the model, demonstrating the key features, is shown in Figure 3.7.

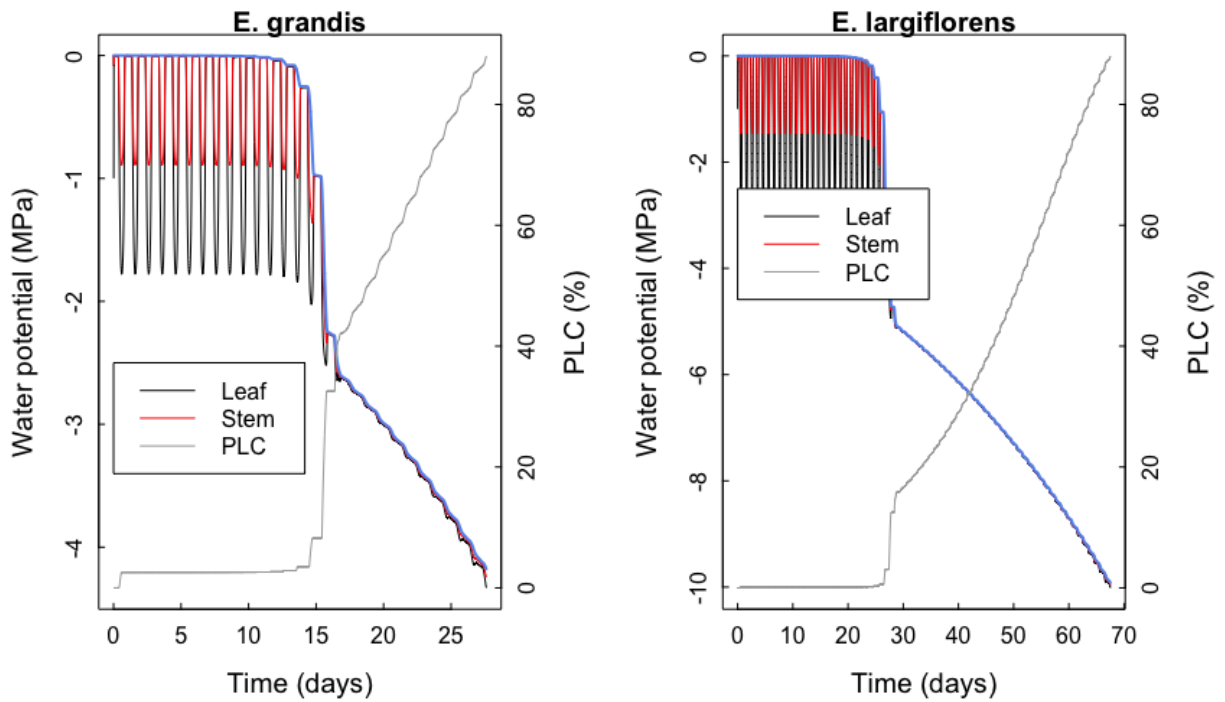


Figure 3.7. Output from a simplified version of the model is demonstrated for two contrasting species, assumed to be growing in 75 L pots as in Experiment 2. The figures show leaf, stem and soil water potential (black, red and blue lines, respectively) and the percent loss of conductivity of the stem (PLC%). The two phases of the dry down can be seen clearly: the first phase shows leaf water potential dropping during the day as the transpiration stream causes water to be lost from the plant and refilling at night when stomata close, while the second phase shows plant water potential dropping gradually as the plant desiccates. The predicted time to mortality increases as a function of the species traits.

4. Remote Sensing / Monitoring

We had intended to use a remote sensing approach to identify mortality, as has been done elsewhere (e.g. Anderegg et al. 2015). However, the CI due to undertake this work (Brad Evans) moved to another institution at the start of the project and was unable to participate. We worked with a sabbatical visitor, Dr Chris Williams from Clarke University, to examine available data during the Millennium Drought. We examined remotely-sensed measures of the fraction of absorbed PAR, vegetation optical depth, and aboveground biomass carbon during drought and non-drought periods. However, the patchy nature of mortality in Eucalypt-dominated stands make it difficult to identify when analysing regional-scale data. We identified regions of vegetation decline during this period, but were unable to confirm mortality (Tong et al., in review).

In order to increase the number of reliable observations of tree death and better develop our understanding of the conditions under which mortality is likely to occur, we worked with Atlas of Living Australia to set up a “Dead Tree Detective” citizen science site (www.tinyurl.com/deadtreedetective). This site allows scientists and laypeople alike to record photographs of dead trees and comment on potential causes - noting that many episodes of tree mortality in Australian ecosystems can be caused by factors other than drought. Uploads to this site to date show that the current ongoing drought in SE Australia is causing tree death in many locations, from the Qld-NSW border down to Tasmania. The information currently being gathered by this site will be invaluable for future studies of drought-related mortality.

5. General Discussion

Our species distribution modelling approach indicates that future drought mortality risk varies depending on the future climate scenario (Figure 2.2). Drought mortality risk does not increase in climate scenarios where warming is accompanied by increases in precipitation. There is a small increase in risk where there is no change in precipitation, and a large increase in risk where precipitation is projected to decline.

The analysis highlights that there is drought risk across the state, but the risk appears to be concentrated along the Great Dividing Range, with particular hotspots inland from Sydney and Newcastle (Figure 2.3). This region contains a relatively large number of common species projected to move out of their current hydric envelopes.

We also used the species distribution approach to identify locations likely to have experienced dry stress during the Millennium Drought. Our aim in carrying out this analysis was to test the approach against observations of drought mortality in the recent past; however, this test was made difficult by a lack of suitable observations. As noted in Section 4, we were unable to use remotely-sensed data as originally planned. We were able to confirm dry stress predictions against the limited dataset of mortality observations recorded on the ground during the Millennium Drought. During this period in NSW, there

are confirmed records of tree mortality for *E. delegatensis* near Tumbarumba (Keith et al. 2012), and *E. viminalis* near Cooma (Ross & Brack 2015) and anecdotal reports of tree death of *Eucalyptus macrorhyncha* near Cowra and *E. populnea* near Cobar (Semple et al. 2010) - all of which are highlighted by the analysis (Appendix 4). However, the analysis also highlights dry stress for a number of other species for which there are no observations of tree death. Owing to the lack of records, it is unclear whether tree death occurred for these species in these locations or not. Future studies of drought stress will be greatly facilitated by the Dead Tree Detective citizen science website that we established (Section 4).

Although it may appear that drought mortality risk was higher during the Millennium Drought than projected for the future (Table 2.2), we caution strongly against this conclusion, for several reasons. Firstly, the NARCLIM climate scenarios only represent one realisation of each climate model, and do not capture the risk of extreme drought during this period. The baseline period 1990-2010, for example, does not capture the Millennium Drought. Risk of extremes is not well captured by climate models at present, but is a subject of ongoing research in the current ARC Centre of Excellence for Climate Extremes. Secondly, the species distribution approach was applied on a twenty-year timescale for the future periods, examining whether the species had moved out of its hydrological envelope on average during the twenty years. The appropriate timescale for tree mortality remains unclear. Anecdotal observations over the last 18 months, which have seen a historically low rainfall in NSW, suggest greater tree mortality during this period than during the more extended, but less severe, drought over the Millennium Drought period. The ecophysiological data and models developed in this project provide a solid basis for us to estimate the timescale and severity of drought that are likely to cause mortality in species growing in different parts of NSW and thus develop this research further.

References

Adams HD, Zeppel MJB, Anderegg WRL, Hartmann H, Landhäusser SM, Tissue DT, Huxman TE, Hudson PJ, Franz TE, Allen CD, Anderegg LDL, Barron-Gafford GA, Beerling DJ, Breshears DD, Brodribb TJ, Bugmann H, Cobb RC, Collins AD, Dickman LT, Duan H, Ewers BE, Galiano L, Galvez DA, Garcia-Forner N, Gaylord ML, Germino MJ, Gessler A, Hacke UG, Hakamada R, Hector A, Jenkins MW, Kane JM, Kolb TE, Law DJ, Lewis JD, Limousin J-M, Love DM, Macalady AK, Martínez-Vilalta, J, Mencuccini, M, Mitchell, PJ, Muss, JD, O'Brien, MJ, O'Grady, AP, Pangle, RE, Pinkard, EA, Piper, FI, Plaut, JA, Pockman, WT, Quirk, J, Reinhardt, K, Ripullone, F, Ryan, MG, Sala, A, Sevanto, S, Sperry, JS, Vargas, R, Vennetier, M, Way, DA, Xu, C, Yopez, EA & McDowell, NG (2017) A multi-species synthesis of physiological mechanisms in drought-induced tree mortality. *Nature Ecology & Evolution*, 1: 1285-1291.

Anderegg WRL, Flint A, Huang C-y, Flint L, Berry JA, Davis Frank W, Sperry JS & Field CB (2015) Tree mortality predicted from drought-induced vascular damage. *Nature Geoscience*, 8: 367-371.

Blackman, CJ, Pfautsch, S, Choat, B, Delzon, S, Gleason, SM, and Duursma, R A (2016) Toward an index of desiccation time to tree mortality under drought. *Plant, Cell & Environment*, 39: 2342–2345. doi: 10.1111/pce.12758.

Blackman CJ, Creek D, Maier C, Aspinwall MJ, Drake JE, Pfautsch S, O'Grady A, Delzon S, Medlyn BE, Tissue DT & Choat B (2019) Drought response strategies and hydraulic traits contribute to mechanistic understanding of plant dry-down to hydraulic failure. <https://doi.org/10.1093/treephys/tpz016>

Blackman CJ, Li X, Choat B, Rymer P, De Kauwe MG, Duursma RA, Tissue DT & Medlyn BE (in review) Plant desiccation time is highly predictable across eight eucalypts from contrasting climates.

Charrier G, Torres-Ruiz JM, Badel E, Burlett R, Choat B, Cochard H, Delmas CEL, Domec J-C, Jansen S, King A, Lenoir N, Martin-StPaul N, Gambetta GA & Delzon S (2016) Evidence for Hydraulic Vulnerability Segmentation and Lack of Xylem Refilling under Tension. *Plant Physiology*, 172: 1657-1668.

Choat B, Brodribb TJ, Brodersen CR, Duursma RA, Lopez R & Medlyn BE (2018) Triggers of tree mortality under drought. *Nature*, 558: 531–539.

Choat B, Brodersen CR & McElrone AJ (2015) Synchrotron X-ray microtomography of xylem embolism in *Sequoia sempervirens* saplings during cycles of drought and recovery. *New Phytologist*, 205: 1095-1105.

Choat B, Jansen S, Brodribb TJ, Cochard H, Delzon S, Bhaskar R, Bucci SJ, Field TS, Gleason SM, Hacke UG, Jacobsen AL, Lens F, Maherali H, Martínez-Vilalta J, Mayr S, Mencuccini M, Mitchell PJ, Nardini A, Pittermann J, Pratt RB, Sperry JS, Westoby M, Wright IJ & Zanne AE (2012) Global convergence in the vulnerability of forests to drought. *Nature*, 491: 752-755.

Drake JE, Power SA, Duursma RA, Medlyn BE, Aspinwall MJ, Choat B, Creek D, Eamus D, Maier C, Pfautsch S, Smith RA, Tjoelker MG & Tissue DT (2018) Stomatal and non-stomatal limitations of photosynthesis for four tree species under drought: a comparison of model formulations. *Agricultural and Forest Meteorology*, 247:454-466.

Dewar RC, Mauranen A, Makela A, Holtta T, Medlyn BE & Vesala T (2018) New insights into the covariation of stomatal, mesophyll and hydraulic conductances from optimisation models incorporating non-stomatal limitations to photosynthesis. *New Phytologist*, 217: 571-585

Elith J & Leathwick J (2009) Species distribution models; ecological explanation and prediction across space and time. *Annual Review of Ecology, Evolution, and Systematics*, 40: 677-697.

Franklin J (2010) *Mapping species distributions: spatial inference and prediction*. Cambridge University Press.

Evans J P, Ji F, Lee C, Smith P, Argüeso D & Fita L (2014) Design of a regional climate modelling projection ensemble experiment–NARClIM. *Geoscientific Model Development*, 7: 621-629.

Hutchinson M & Xu T (2014) Methodology for generating Australia-wide surfaces and associated grids for monthly mean daily maximum and minimum temperature, rainfall, pan evaporation and solar radiation for the periods 1990–2009, 2020–2039 and 2060–2079. *NARClIM Report to the NSW Office of Environment and Heritage*.

Keith D (2004) *Ocean shores to desert dunes: the native vegetation of New South Wales and the ACT*. NSW Department of Environment and Conservation, Sydney, Australia.

Keith H, van Gorsel E, Jacobsen KL & Cleugh HA (2012) Dynamics of carbon exchange in a Eucalyptus forest in response to interacting disturbance factors. *Agricultural and Forest Meteorology* 153: 67-81.

Li X, Blackman CJ, Choat B, Duursma RA, Rymer PD, Medlyn BE & Tissue DT (2018a) Tree hydraulic traits are co-ordinated and strongly linked to climate-of-origin across a rainfall gradient. *Plant, Cell and Environment*, 41: 646-660.

Li X, Blackman CJ, Rymer PD, Quintans D, Duursma RA, Choat B, Medlyn BE & Tissue DT (2018b) Xylem embolism measured retrospectively is linked to canopy dieback in natural populations of *Eucalyptus piperita* following drought. *Tree Physiology*, 38: 1193-1191.

Li X, Blackman CJ, Choat B, Rymer PD, Medlyn BE & Tissue DT (2019a) Drought tolerance traits do not vary across sites differing in water availability in *Banksia serrata* (Proteaceae). *Functional Plant Biology* <https://doi.org/10.1071/FP18238>

Li X, Blackman CJ, Peters JMR, Choat B, Rymer PD, Medlyn BE & Tissue DT (2019b) More than iso/anisohydry: hydroscares integrate plant water-use and drought tolerance traits in ten eucalypt species from contrasting climates. *Functional Ecology* <https://doi.org/10.1111/1365-2435.13320>.

McDowell N, Pockman WT, Allen CD, Breshears DD, Cobb N, Kolb T, Plaut J, Sperry J, West A, Williams DG & Yepez EA (2008) Mechanisms of plant survival and mortality during drought: why do some plants survive while others succumb to drought? *New Phytologist*, 178, 719-739.

Mitchell PJ, O'Grady AP, Hayes KR & Pinkard EA (2014) Exposure of trees to drought-induced die-off is defined by a common climatic threshold across different vegetation types. *Ecology and Evolution* 4(7): 1088-1101.

Meehl GA, Stocker TF, Collins WD, Friedlingstein P, Gaye AT, Gregory JM, Kitoh A, Knutti R, Murphy JM, Noda A, Raper SCB, Watterson IG, Weaver AJ & Zhao Z-C (2007) *Global Climate Projections. Climate Change 2007: The Physical Science Basis*. Contribution of Working Group I to the Fourth Assessment Report of the Intergovernmental Panel on Climate Change (ed. by S Solomon, D Qin, M Manning, Z Chen, M Marquis, KB Averyt, M Tignor and HL Miller). Cambridge University Press, Cambridge, United Kingdom and New York, NY, USA.

Meinzer FC & McCulloh KA (2013) Xylem recovery from drought-induced embolism: where is the hydraulic point of no return? *Tree Physiology*, 33, 331-334.

Nakicenovic N, Alcamo J, Davis G, deVries B, Fenhann J, Gaffin S, Gregory K, Grubler A, Jung T-Y, Kram T, LaRovere E, Michaelis L, Mori S, Morita T, Pepper W, Pitcher H, Price L, Riahi K, Roehrl A, Rogner H-H, Sankovski A, Schlesinger M, Shukla P, Smith S, Swart R, vanRooijen S, Victor N & Dadi Z (2000) *IPCC Special Report on Emissions Scenarios*. In, p. 599. Cambridge University Press, UK, Cambridge.

Nicholls N, Drosowsky W & Lavery B. (1997) Australian rainfall variability and change. *Weather*, 52: 66-72. doi:10.1002/j.1477-8696.1997.tb06274.x

Ogasa M, Miki NH, Murakami Y & Yoshikawa K (2013) Recovery performance in xylem hydraulic conductivity is correlated with cavitation resistance for temperate deciduous tree species. *Tree Physiology*, 33: 335-344.

R Development Core Team, 2014. *R: A language and environment for statistical computing* 3.1.2, R Foundation for Statistical Computing, Vienna, Austria.

Ross C & Brack C (2015) *Eucalyptus viminalis* dieback in the Monaro region, NSW. *Australian Forestry*, 78: 243-253, DOI: [10.1080/00049158.2015.1076754](https://doi.org/10.1080/00049158.2015.1076754)

Semple B, Rankin M, Koen T & Geeves G (2010) A Note on Tree Deaths during the Current (2001–?) Drought in South-eastern Australia. *Australian Geographer*, 41: 391-401, DOI: [10.1080/00049182.2010.498042](https://doi.org/10.1080/00049182.2010.498042)

Skamarock WC, Klemp JB, Dudhia J, Gill DO, Barker DM, Duda M, Huang XY, Wang W & Powers JG (2008) *A description of the advanced research WRF version 3*. NCAR Technical Note, National Center for Atmospheric Research, Boulder, CO, USA.

Sperry JS, Venturas MD, Anderegg WRL, Mencuccini M, Mackay DS, Wang Y & Love DM (2017) Predicting stomatal responses to the environment from the optimization of photosynthetic gain and hydraulic cost. *Plant, Cell & Environment*, 40: 816–830. doi: 10.1111/pce.12852.

Tong J, Williams Ca, Rogan J, Medlyn BE & De Kauwe MG (in review) Drought impacts on Australian vegetation during the Millennium Drought measured with multi-source spaceborne remote sensing.

van Dijk AIJM, Beck HE, Crosbie RS, de Jeu RAM, Liu YY, Podger GM, Timbal B, & Viney NR (2013) The Millennium Drought in southeast Australia (2001–2009): Natural and human causes and implications for water resources, ecosystems, economy, and society. *Water Resources Research*, 49: 1040-1057.

Appendix 1. Scientific Publications to Date

Blackman CJ, Creek D, Maier C, Aspinwall MJ, Drake JE, Pfautsch S, O’Grady A, Delzon S, Medlyn BE, Tissue DT & Choat B (2019) Drought response strategies and hydraulic traits contribute to mechanistic understanding of plant dry-down to hydraulic failure. <https://doi.org/10.1093/treephys/tpz016>

Blackman CJ, Li X, Choat B, Rymer P, De Kauwe MG, Duursma RA, Tissue DT & Medlyn BE (in review) Plant desiccation time is highly predictable across eight eucalypts from contrasting climates.

Choat B, Brodribb TJ, Brodersen CR, Duursma RA, Lopez R & Medlyn BE (2018) Triggers of tree mortality under drought. *Nature* 558: 531–539.

De Kauwe MG, Medlyn BE, Knauer J & Williams CA (2017) Ideas and perspectives: How coupled is the vegetation to the boundary layer? *Biogeosciences*, 14, 4435-4453.

Duursma RA, Blackman C, López R, Martin-StPaul N, Cochard H & Medlyn BE (2018) Tansley Review: On the minimum leaf conductance: its role in models of plant water use, and ecological and environmental controls. *New Phytologist* 221: 693-705.

Li X, Blackman CJ, Choat B, Duursma RA, Rymer PD, Medlyn BE & Tissue DT (2018a) Tree hydraulic traits are co-ordinated and strongly linked to climate-of-origin across a rainfall gradient. *Plant, Cell and Environment*, <https://doi.org/10.1111/pce.13129>

Li X, Blackman CJ, Rymer PD, Quintans D, Duursma RA, Choat B, Medlyn BE & Tissue DT (2018b) Xylem embolism measured retrospectively is linked to canopy dieback in natural populations of *Eucalyptus piperita* following drought. *Tree Physiology* <https://doi.org/10.1093/treephys/tpy052>

Li X, Blackman CJ, Choat B, Rymer PD, Medlyn BE & Tissue DT (2019a) Drought tolerance traits do not vary across sites differing in water availability in *Banksia serrata* (Proteaceae). *Functional Plant Biology* <https://doi.org/10.1071/FP18238>

Li X, Blackman CJ, Peters JMR, Choat B, Rymer PD, Medlyn BE & Tissue DT (2019b) More than iso/anisohydry: hydroscares integrate plant water-use and drought tolerance traits in ten eucalypt species from contrasting climates. *Functional Ecology* <https://doi.org/10.1111/1365-2435.13320>.

Tong J, Williams Ca, Rogan J, Medlyn BE & De Kauwe MG (in review) Drought impacts on Australian vegetation during the Millennium Drought measured with multi-source spaceborne remote sensing.

Ukkola AM, De Kauwe MG, Pitman AJ, Best MJ, Haverd V, Decker M, Abramowitz G & Haughton N (2016) Land surface models systematically overestimate the intensity, duration and magnitude of seasonal-scale evaporative droughts. *Environmental Research Letters*, 11, 104012.

Ukkola A, Houghton N, De Kauwe MG, Abramowitz G & Pitman A (2017) FluxnetLSM R package (v1.0): A community tool for processing FLUXNET data for use in land surface modelling. *Geoscientific Model Development*, 10, 3379-3390.

Ukkola AM, Pitman AJ, Decker M, Abramowitz G, De Kauwe MG, Kala J & Wang Y-P (2016) Modelling evapotranspiration during precipitation deficits: identifying critical processes in a land surface model. *Hydrological and Earth System Sciences*, 20, 2403-2419.

Appendix 2. Hydric envelope for 47 tree species

Hydric envelopes were calculated a Climate Moisture Index (precipitation minus potential transpiration) for the period 1970-2000, derived from AWAP data. The percentiles of the envelope were quantified from the set of unique 1 km x 1 km grid cells for which occurrences of each species were available in the Atlas of Living Australasia. Vegetation classes: RF = rainforest, DSF = dry sclerophyll forest, SAW = semi-arid woodland, GW = grass woodland, ALP = alpine, WSF = wet sclerophyll forest.

Family	Species	Veg class	n cells (Aus)	n cells (NSW)	Baseline hydric envelope				
					0%	2.50%	50%	97.50%	100%
Antherospermataceae	<i>Doryphora sassafras</i>	RF	1704	1692	-623.4	-409.1	8.6	795.0	1340.1
Casuarinaceae	<i>Allocasuarina torulosa</i>	DSF	4966	4594	-1060.3	-655.9	-177.1	464.2	1347.6
Casuarinaceae	<i>Casuarina pauper</i>	SAW	2852	890	-1754.0	-1586.7	-1283.4	-1069.2	-857.1
Cunoniaceae	<i>Ceratopetalum apetalum</i>	RF	1606	1598	-671.8	-455.2	-24.1	913.5	1340.1
Cupressaceae	<i>Callitris glaucophylla</i>	SAW	8026	6078	-1707.4	-1556.5	-940.5	-607.6	213.4
Fabaceae	<i>Acacia aneura</i>	SAW	4022	495	-1862.9	-1734.0	-1534.9	-1218.6	-982.3
Fabaceae	<i>Acacia harpophylla</i>	SAW	701	316	-1537.0	-1373.1	-1011.6	-586.4	304.4
Fabaceae	<i>Acacia melanoxylon</i>	RF	16515	4450	-1105.9	-586.8	-221.1	575.2	1823.1
Fabaceae	<i>Acacia melvillei</i>	SAW	477	286	-1495.8	-1349.6	-1100.2	-824.4	-534.8
Myrtaceae	<i>Angophora costata</i>	DSF	2784	2760	-1261.2	-590.6	-154.6	233.3	654.4
Myrtaceae	<i>Angophora floribunda</i>	GW	6412	6148	-1240.0	-900.5	-490.5	20.0	1956.3
Myrtaceae	<i>Corymbia gummifera</i>	DSF	3827	3749	-853.0	-486.8	-136.7	310.5	1212.4
Myrtaceae	<i>Eucalyptus albens</i>	DSF	4361	3876	-1206.8	-893.4	-690.3	-375.1	763.7
Myrtaceae	<i>Eucalyptus blakelyi</i>	GW	2971	2844	-1126.9	-899.8	-591.7	-300.1	297.7
Myrtaceae	<i>Eucalyptus bridgesiana</i>	GW	3372	2586	-945.9	-676.9	-443.7	-15.4	806.6
Myrtaceae	<i>Eucalyptus camaldulensis</i>	SAW	14433	3414	-1932.1	-1671.6	-812.6	-354.7	400.6
Myrtaceae	<i>Eucalyptus coolabah</i>	SAW	2930	1489	-1822.2	-1785.5	-1341.8	-987.1	-732.6
Myrtaceae	<i>Eucalyptus crebra</i>	DSF	6051	3821	-1501.8	-1240.0	-753.7	-48.2	1899.0
Myrtaceae	<i>Eucalyptus cypellocarpa</i>	WSF	5039	1876	-868.3	-456.0	-119.8	579.0	1013.5
Myrtaceae	<i>Eucalyptus dalrympleana</i>	WSF	3015	2248	-929.8	-528.5	-152.2	690.2	1611.1
Myrtaceae	<i>Eucalyptus deanei</i>	WSF	846	839	-830.4	-613.8	-349.3	48.2	306.8
Myrtaceae	<i>Eucalyptus delegatensis</i>	WSF	4533	370	-589.6	-269.7	279.9	1370.2	2198.3
Myrtaceae	<i>Eucalyptus dumosa</i>	SAW	4526	1338	-1531.3	-1298.0	-1103.8	-834.6	-529.5
Myrtaceae	<i>Eucalyptus grandis</i>	WSF	926	757	-859.0	-368.8	62.3	786.2	1349.7
Myrtaceae	<i>Eucalyptus largiflorens</i>	SAW	2146	1489	-1607.4	-1392.2	-1105.0	-789.7	-478.3
Myrtaceae	<i>Eucalyptus macroryncha</i>	GW	6759	3528	-1169.4	-768.6	-434.5	46.4	1379.6
Myrtaceae	<i>Eucalyptus melliodora</i>	GW	3961	3266	-1101.5	-965.8	-558.3	-203.9	531.4
Myrtaceae	<i>Eucalyptus microcorys</i>	WSF	3860	3507	-994.1	-459.5	-54.4	522.1	1124.6
Myrtaceae	<i>Eucalyptus moluccana</i>	DSF	2762	2330	-1261.1	-948.2	-518.9	-113.9	2303.3
Myrtaceae	<i>Eucalyptus obliqua</i>	WSF	9512	1387	-860.8	-519.9	-160.6	478.4	2472.3
Myrtaceae	<i>Eucalyptus pauciflora</i>	ALP	3231	1990	-957.4	-535.8	-166.6	1010.4	1611.1
Myrtaceae	<i>Eucalyptus pilularis</i>	WSF	3650	3379	-919.0	-460.8	-34.0	483.6	1347.6
Myrtaceae	<i>Eucalyptus populnea</i>	SAW	2287	1875	-1601.0	-1431.2	-1035.0	-845.5	472.5
Myrtaceae	<i>Eucalyptus racemosa</i>	DSF	2186	1971	-658.9	-523.0	-131.3	347.8	1212.4
Myrtaceae	<i>Eucalyptus rossii</i>	DSF	1600	1600	-931.7	-805.6	-515.6	-199.9	384.1
Myrtaceae	<i>Eucalyptus saligna</i>	WSF	2798	2697	-1011.5	-538.0	-145.4	443.4	901.7
Myrtaceae	<i>Eucalyptus sideroxylon</i>	DSF	1034	975	-1154.1	-1044.5	-779.9	-350.9	-3.4
Myrtaceae	<i>Eucalyptus teretecornis</i>	DSF	5395	4124	-1280.8	-995.6	-399.8	202.9	1391.4
Myrtaceae	<i>Eucalyptus viminalis</i>	WSF	13987	2631	-1117.1	-632.1	-258.7	499.5	1676.5
Myrtaceae	<i>Syncarpia glomulifera</i>	WSF	4568	4252	-1224.1	-559.1	-83.2	461.8	2635.8
Myrtaceae	<i>Syzygium smithii</i>	RF	270	109	-965.9	-493.6	-142.5	672.3	1773.0
Myrtaceae	<i>Tristaniopsis laurina</i>	RF	1726	1312	-877.9	-541.4	-140.0	653.4	1320.0
Nothofagaceae	<i>Nothofagus moorei</i>	RF	271	271	-375.4	-236.9	257.5	928.2	1432.8
Pittosporaceae	<i>Pittosporum undulatum</i>	RF	7658	5387	-929.6	-576.6	-171.8	491.9	1320.0
Proteaceae	<i>Banksia serrata</i>	DSF	4458	3196	-647.5	-512.2	-132.8	290.7	1301.4
Proteaceae	<i>Hakea leucoptera</i>	SAW	1769	462	-1820.4	-1788.9	-1350.3	-926.2	-700.9
Sapindaceae	<i>Alectryon oleifolius</i>	SAW	5071	2091	-1924.1	-1626.3	-1200.5	-836.5	-561.7

Appendix 3. Dry stress for NSW/ACT stands of 47 tree species

For each species, the number of stands (defined as 1 km x 1 km grid cells within NSW/ACT with at least one occurrence record in the Atlas of Living Australia) with values below the 2.5th percentile of the species' hydric envelope (see Appendix 2) were summed for a number of time periods: pre-drought baseline (1970-2000), during the Millennium Drought (2001-2009), scenarios from four global climate models within NARCLIM for 2030 and 2070. ALL refers to stands projected to be moisture stressed under all of the NARCLIM scenarios for that time period.

Species	N stands under stress											
	Pre-drought	During drought	2030					2070				
			CCCMA	CSIRO	ECHAM	MIROC	ALL	CCCMA	CSIRO	ECHAM	MIROC	ALL
<i>Doryphora sassafras</i>	42	223	13	102	46	8	7	17	124	23	3	3
<i>Allocasuarina torulosa</i>	49	181	27	143	46	16	16	21	143	39	4	4
<i>Casuarina pauper</i>	1	18	0	1	0	0	0	0	1	0	0	0
<i>Ceratopetalum apetalum</i>	41	179	8	93	49	9	6	13	83	18	2	2
<i>Callitris glaucophylla</i>	2	17	2	2	2	0	0	2	3	1	0	0
<i>Acacia aneura</i>	0	0	0	0	0	0	0	0	0	0	0	0
<i>Acacia harpophylla</i>	0	92	0	73	0	0	0	0	21	0	0	0
<i>Acacia melanoxylon</i>	72	425	45	156	119	31	30	38	157	70	12	12
<i>Acacia melvillei</i>	11	47	1	24	1	0	0	4	22	1	0	0
<i>Angophora costata</i>	55	258	4	156	53	5	4	6	143	10	1	1
<i>Angophora floribunda</i>	55	243	21	149	39	4	4	4	183	32	1	1
<i>Corymbia gummifera</i>	81	692	10	297	86	9	7	17	195	20	6	6
<i>Eucalyptus albens</i>	90	784	11	319	28	6	6	8	317	17	0	0
<i>Eucalyptus blakelyi</i>	75	358	20	207	64	14	12	19	218	48	2	2
<i>Eucalyptus bridgesiana</i>	83	985	34	214	175	22	19	24	240	86	3	2
<i>Eucalyptus camaldulensis</i>	0	9	0	0	0	0	0	0	0	0	0	0
<i>Eucalyptus coolabah</i>	0	0	0	0	0	0	0	0	0	0	0	0
<i>Eucalyptus crebra</i>	0	0	0	0	0	0	0	0	0	0	0	0
<i>Eucalyptus cypellocarpa</i>	105	536	62	143	124	37	37	51	147	75	8	8
<i>Eucalyptus dalrympleana</i>	69	392	28	223	80	13	11	14	256	87	0	0
<i>Eucalyptus deanei</i>	19	153	3	109	14	3	3	3	157	6	1	1
<i>Eucalyptus delegatensis</i>	12	82	10	16	18	12	10	11	43	12	16	11
<i>Eucalyptus dumosa</i>	80	634	8	219	192	80	6	26	109	159	0	0
<i>Eucalyptus grandis</i>	15	61	3	37	12	4	3	4	23	8	4	4
<i>Eucalyptus largiflorens</i>	34	225	21	82	26	16	13	31	72	20	6	6
<i>Eucalyptus macroryncha</i>	147	553	48	304	156	44	38	43	304	102	27	27
<i>Eucalyptus melliodora</i>	93	415	26	182	139	19	13	25	166	68	2	2
<i>Eucalyptus microcorys</i>	44	299	6	163	42	8	5	18	180	26	4	4
<i>Eucalyptus moluccana</i>	1	19	0	7	1	0	0	0	12	0	0	0
<i>Eucalyptus obliqua</i>	10	28	6	18	10	4	4	5	43	10	1	1
<i>Eucalyptus pauciflora</i>	78	378	48	168	149	26	25	46	149	58	2	2
<i>Eucalyptus pilularis</i>	42	307	3	158	61	8	2	22	95	13	2	2
<i>Eucalyptus populnea</i>	25	69	3	31	7	2	2	5	32	2	0	0
<i>Eucalyptus racemosa</i>	47	416	1	143	68	2	0	4	111	5	0	0
<i>Eucalyptus rossii</i>	40	133	2	79	29	2	2	2	78	33	0	0
<i>Eucalyptus saligna</i>	33	204	6	117	36	6	6	7	103	19	3	3
<i>Eucalyptus sideroxylon</i>	24	270	5	54	30	1	1	4	54	11	0	0
<i>Eucalyptus teretecomis</i>	0	2	0	0	0	0	0	0	0	0	0	0
<i>Eucalyptus viminalis</i>	49	467	11	160	86	8	7	4	128	22	5	2
<i>Syncarpia glomulifera</i>	59	419	0	229	58	3	0	5	156	4	0	0
<i>Syzygium smithii</i>	2	13	1	5	1	1	1	1	6	1	1	1
<i>Tristaniopsis laurina</i>	36	165	5	68	42	5	4	8	57	10	2	2
<i>Nothofagus moorei</i>	7	11	1	24	4	0	0	0	23	4	0	0
<i>Pittosporum undulatum</i>	147	513	69	305	160	54	49	67	303	103	16	15
<i>Banksia serrata</i>	29	340	1	104	41	2	1	11	58	12	0	0
<i>Hakea leucoptera</i>	0	0	0	0	0	0	0	0	0	0	0	0
<i>Alectryon oleifolius</i>	0	17	0	0	0	0	0	0	0	0	0	0

Appendix 4. Maps of dry stress for 47 tree species

The following maps illustrate locations of known stands of 47 NSW/ACT tree species (based on data from the Atlas of Living Australasia, at a spatial resolution of 10 km). Grid cells are colour-coded, illustrating a) orange: stands subjected to dry stress in the pre-drought period 1970-2000 and during the Millennium Drought (2001-2009), b) dark blue: stands subjected to dry stress in the pre-drought period only, c) red: stands subjected to dry stress during the Millennium Drought and d) light blue: unstressed in either time period. See Section 2 for the definition of dry stress.

